ORIGINAL ARTICLE

Interplay of anthropogenic and natural drivers of observed coupled sea surface temperature - Arctic sea ice variability

Petru Vaideanu[1,2,4] · Mihai Dima[1,2] · Denis-Raducu Nichita[2,3] · Christian Stepanek[1] · Paul Gierz[1] · Norel Rimbu[1] · Monica Ionita[1,4] · Gerrit Lohmann[1,5]

Abstract

Arctic sea ice plays a pivotal role in shaping the climate system at high latitudes, acting as both an indicator and driver of climate change processes in this sensitive region. Its seasonal variability and long-term decline have far-reaching implications for global climate dynamics, regional ecosystems, and human activities. While climate models indicate clear evidence of human-induced sea ice decline, quantification of the relative contributions of forcing factors in relation to climate-system internal processes remains uncertain. Here, we tackle this uncertainty by employing a combination of statistical analyses on observational data, highlighting the distinct fingerprints of increased atmospheric CO_2 concentration as external forcing, the Atlantic Multidecadal Oscillation (AMO) as well as the North Atlantic Oscillation (NAO), as modes of internal variability, on global sea surface temperature (SST) and Arctic sea ice concentration (SIC) since 1950. Our analyses reveal that rising atmospheric CO_2 concentrations are by far the dominant causal factor for SIC variability, while AMO and NAO also play a significant role in either exacerbating or mitigating sea ice loss. Since mid-1980s, the positive trend of the AMO has amplified the declining trend in Arctic sea ice, with its effects being roughly half as large as the effect of rising CO_2 concentrations. Linear regression analyses shed light on the physical processes linking the drivers of Arctic sea ice decline both during phases of sea-ice accumulation and melting. Causal links between increasing atmospheric CO_2 concentrations, the AMO, the NAO, on the one hand, and observed global SST—Arctic SIC patterns on the other are also established. Observation-based coupled SST-SIC interactions underline the past evolution of Arctic sea ice and emphasize the important roles of these drivers in shaping its current and future evolution.

Keywords Sea ice · Climate change · CO_2 increase · AMO · NAO · Sea surface temperature · Arctic · CCA · CCM · Observations

1 Introduction

Arctic sea ice stands as a crucial element for our climate. It influences the vertical structure of the Arctic Ocean (Zhong et al. 2022), impacts deep-water formation and overturning (Bretones et al. 2022), modulates the exchange of heat and momentum between ocean and atmosphere in the Arctic scales (Kattsov et al. 2011; Döscher et al. 2014), and contributes to polar amplification of temperature change via the ice-albedo feedback (IPCC AR6 WGI 2021). In recent decades, a notable decline in Arctic sea ice has been observed in all seasons (Serreze et al. 2007; Stroeve and Notz 2018) a trend potentially unprecedented in the last approximately 170 years (Walsh et al. 2017). This decrease is largely due to the anthropogenic rise in atmospheric CO_2 concentration (Gillett et al. 2008; Notz and Stroeve 2016; Mueller et al.

✉ Petru Vaideanu
  petru.cosmin.vaideanu@awi.de

1 Alfred Wegener Institute Helmholtz Centre for Polar and Marine Research, Bremerhaven, Germany

2 Faculty of Physics, University of Bucharest, Bucharest-Măgurele, Romania

3 "Horia Hulubei" National Institute of Physics and Nuclear Engineering, Bucharest-Măgurele, Romania

4 Faculty of Forestry, Stefan Cel Mare University, Suceava, Romania

5 MARUM & Department of Environmental Physics, University of Bremen, Bremen, Germany

2018). Without a gradual reduction in carbon emissions, climate models show that the Arctic Ocean will be practically free of sea ice in summer in the next few decades (Notz and Stroeve 2018). A partially sea-ice free Arctic during summer has been proposed as a characteristic of the Earth system during the Last Interglacial (Vermassen et al. 2023) and the Miocene (Stein et al. 2016) highlighting the extent and rarity of the climate processes currently underway. However, it is important to recognize that natural variability has a significant role in the Arctic's sea ice evolution on a range of time scales (e.g., from interannual to millennial). This has been based on proxy records (Fauria et al. 2010), historical records (Divine and Dick 2006; Miles et al. 2014), observations (Ding et al. 2014; Chen et al. 2016; Yu et al. 2017; Cai et al. 2021a; Ionita 2023; Vaideanu et al. 2023b) and model simulations (Kay et al. 2011; Swart et al. 2015; England et al. 2019).

The Atlantic Multidecadal Oscillation (AMO) (Schlesinger and Ramankutty 1994; Kerr 2000) is the dominant mode of multidecadal variability in the North Atlantic and has a global influence on climate (Sutton and Hodson 2005; Ruprich-Robert et al. 2017; Vaideanu et al. 2018). The AMO has traditionally been previously linked to the variations of the ocean circulation, which is based on climate models (Latif et al. 2004; Jungclaus et al. 2005; Knight et al. 2005; Wei and Lohmann 2012), and observational data (Dima and Lohmann 2007). However, other studies have highlighted the importance of external factors, such as solar (Otterå et al. 2010) and volcanic (Otterå et al. 2010; Mann et al. 2021) activities in shaping AMO's behavior. Booth et al. (2012) highlighted the dominant role of anthropogenic aerosols in twentieth-century North Atlantic climate variability, although this hypothesis has been questioned (Zhang et al. 2013). A significant influence of greenhouse gases on the AMO has also been proposed (Bellucci et al. 2017; Murphy et al. 2017; Bellomo et al. 2018). On interannual time scales, the North Atlantic Oscillation (NAO, Hurrell 1995), emerges as the most prominent pattern of North Atlantic atmospheric variability. The NAO is closely related to the Arctic Oscillation (AO) or the Northern Annular Mode (NAM) (Thompson and Wallace 2000), affecting temperature patterns in the North Atlantic sector, in both winter and summer (Folland et al. 2009). Although the spatial pattern of the AO/ NAM is slightly different from the spatial structure of the NAO especially in the North Pacific, the time series of these two modes are strongly correlated (Wang and Ikeda 2001; Wu et al. 2006; Deser et al. 2010).

Both the AMO (Day et al. 2012; Ionita et al. 2019) and NAO (Deser and Teng 2008; Cai et al. 2021a) exert an influence on the Arctic sea ice, mostly through changes in oceanic and atmospheric heat content (Yu et al. 2017; Castruccio et al. 2019; Ding et al. 2019; Olonscheck et al. 2019; Liu et al. 2020). Additionally, Arctic sea ice is also influenced by the atmospheric and oceanic variability in the Pacific Ocean (Screen and Francis 2016; Svendsen et al. 2018). Radiative feedbacks, such as those related to surface albedo (Lei et al. 2016; Kashiwase et al. 2017), water vapor (Curry et al. 1995) and clouds (Letterly et al. 2016), further intensify Arctic warming (Meier et al. 2014; Serreze and Meier 2019; Asbjørnsen et al. 2020). Aerosols, particularly those capable of ice formation, also play a role in modulating radiation reaching the Arctic surface, thereby influencing the energy budget of the region (Creamean et al. 2022). The Barents and Kara Sea regions have shown a significant relationship between sea ice cover and the shortwave cloud radiative effect during summer (Fu et al. 2022).

While the relevance of Arctic sea ice and of its response to enhanced radiative forcing is obvious, it is also noteworthy that there still is a substantial degree of uncertainty regarding the stability of Arctic sea ice in the coming decades and centuries (Cohen et al. 2020). Sources of uncertainty are related to internal variability in the climate system, and to uncertainty in the evolution of the amount of (additional) future radiative forcing, with internal variability dominating uncertainty for the next decade and for climate states with strongly reduced sea ice cover (Bonan et al. 2021).A persistent challenge is the disagreement among models regarding the extent to which recent changes in Arctic sea ice can be attributed to natural versus anthropogenic factors (IPCC AR6 WGI 2021). In this context, observational (instrumental and other observations) data could offer a valuable perspective on recent shifts in Arctic sea-ice. The main goal of this study is to identify, separate and quantify the impact of three different drivers of large-scale changes in coupled sea surface temperature (SST)—sea ice concentration (SIC) variability observed since 1950: the anthropogenic increase in atmospheric CO_2 concentration, the AMO, and the NAO. We also investigate causality between these drivers and the observed coupled SST-SIC patterns. This objective is approached using advanced statistical methods applied on high resolution reconstructed SIC data.

This study is structured as follows: Sect. 2 presents details on the employed observational data and on the methodology applied. Section 3 are presented the results, which are discussed in Sect. 4. Finally, Sect. 5 concludes the paper with an evaluation of the relevance of our work and an outlook on further applications of our findings.

2 Data and methods

2.1 Data

In this section we briefly describe the data sources that we employed towards conducting this study. The observed SIC data has been published by the National Snow and

Ice Data Center (NSIDC), given as percentages of the $0.25 \times 0.25°$-degree area, through the Gridded Monthly Sea Ice dataset Version 2 (Walsh et al. 2017), extending over the 1850–2017 period, available at https://nsidc.org/data/G10010/versions/2. This latest version of the data is based on previous NSIDC products (Walsh and Johnson 1979; Chapman and Walsh 1993), here features improvements on the methodology used to combine various sea-ice observational sources, and advanced gap-filling technique that estimates sea ice in regions, and during months, without any measurement records. Since 1979, the main source of the data is the NSIDC Climate Data Record of Passive Microwave Sea Ice Concentration. Prior to 1979, the sources used to generate gridded data are represented by historical charts of sea ice around Alaska and Denmark, achieves from the Russian Arctic and Antarctic Research Institute and reports from whaling ships (Walsh et al. 2017).

SST data used here is sourced from the National Oceanic and Atmospheric Administration (NOAA) through the Extended Reconstructed Sea Surface Temperature (ErSST. v5) dataset. It is distributed at a $2 \times 2°$ resolution and extends over the period from 1854 to present. The ErSST.v5 dataset benefits from advanced interpolation methods to produce enhanced gridded observations. It can be accessed at https://psl.noaa.gov/data/gridded/data.noaa.ersst.v5.html. Similar results are obtained if the Hadley Centre Sea Ice and Sea Surface Temperature dataset (HadISST, Rayner et al. 2003) is used (not shown).

As a source for surface air temperature (SAT), sea level pressure (SLP), and surface wind, we use outputs from the NOAA NCEP/NCAR Reanalysis data extending from 1948 to present. The NCEP/NCAR Reanalysis project is using a modern analysis/forecast system, where prognostic of climate dynamics are combined with assimilation of surface, satellite, radiosonde, and other observations of key atmospheric variables to create a global data set at a spatial resolution of $2.5 \times 2.5°$ (Kalnay et al. 1996). The NCEP/NCAR Reanalysis data set is available at https://psl.noaa.gov/data/gridded/data.ncep.reanalysis.html.

Previous studies have highlighted the importance of the removing the global-scale climate change signal to derive a robust representation of the AMO (Zhang et al. 2019 and references therein). Therefore, in this study we define and obtain the AMO Index as the second EOF of annual anomalies of Atlantic SST (80ºS to 80ºN) that are derived from the ErSST.v5 dataset after removing the warming trend on a global scale. The NAO Index used here is defined as the 1st EOF of North Atlantic detrended SLP annual anomalies (90–30°W and 0–90°N) from NCEP-NCAR Reanalysis and is publicly available at https://climexp.knmi.nl/data/inao_ncepncar__yr.txt. The atmospheric CO_2 Index measured at Mauna Loa Observatory is obtained from http://www.esrl.noaa.gov/psd/data/climateindices/list/.

Towards performing the analyses presented in this manuscript the following treatment is applied to all data sets. First, the annual cycle is removed from the original time series and monthly anomalies are calculated relative to the 1980–2010 period. Thereafter, annual or seasonal means are computed.

The quality and quantity of observations used to compute the SST (Deser et al. 2010) and SIC (Walsh et al. 2015) data decreases significantly prior to 1950. Therefore, we performed the EOF and CCA analyzes on annual SST-SIC anomalies starting from 1950.

3 Methods

Through the Empirical Orthogonal Functions (EOF) method (Lorenz 1956) applies an orthogonal transformation to convert observational variables into a set of linearly uncorrelated variables. These uncorrelated variables are linear combinations of the original set. Complementary with this, the observed grids are linear combinations of EOFs. If a limited number of EOFs account for a significant portion of the variance, it suggests a simplification of the processes represented in the input data. Essentially, certain climate system variations can be expressed as linear combinations of several EOFs. The primary EOF captures the most variance from the original variables, followed by the second one which accounts for the maximum residual variance, and so on. Given its ability to distinguish patterns, EOF analysis is used at examining the spatial and temporal variability of extensive time series. Here, we used the EOF method on SST and SIC data, in order to increase the signal-to-noise ratio in the two fields.

Canonical Correlation Analysis (CCA) is a multivariate statistical technique used to identify pairs of patterns with maximum correlation between their associated time series (Storch and Zwiers 1999; Levine and Wilks 2000) based on the distinction between time evolutions of patterns (where the time series of consecutive pairs are uncorrelated). In other words, CCA determines the extent to which two structures, each associated with a variable of the initial pairs of fields, are linked. Mathematically, CCA identifies two sets of vectors (one vector for each considered variable) in a way that the correlations between the projections of the variables onto these vectors are mutually maximized (Cherry 1996). Given two sets of variables $X = (x_1, x_2, …, x_n)$ and $Y = (y_1, y_2, …, y_n)$ the goal of CCA is to find linear combinations of variables X and Y, $U_i = \alpha_i^T X$ and $V_i = \beta_j^T X$, that maximize the correlation $< UiVi >$. To accomplish this, sample covariance matrices, Cxx and Cyy, are constructed for X and Y, respectively, capturing the variability within each dataset. The cross-covariance matrix, C_{xy}, represents the covariance between variables X and Y. The canonical correlations are

determined by solving the following coupled eigenproblem with the same eigenvalues, $\lambda 2$:

$$\begin{cases} [C_{xx}]^{-1}[C_{xy}][C_{yy}]^{-1}[C_{yx}]W_x = \rho^2 W_x \\ [C_{yy}]^{-1}[C_{yx}][C_{xx}]^{-1}[C_{xy}]W_y = \rho^2 W_y \end{cases} \quad (1)$$

The eigenvalue λi^2 is equivalent to the squared correlation $< U_i V_i >^2$ (von Storch and Zwiers 1999; Zorita et al. 1992). The pair of eigenfunctions α_1 and β_1 that is associated with the largest eigenvalue represents the maximum correlation between U_1 and V_1.

In order to avoid degeneracy of the covariance matrix we reduce the number of degrees of freedom prior to CCA (Zorita et al. 1992; Cherry 1996). Therefore, in CCA, the new variables introduced are the time series of EOFs, with an equal number of eigenmodes for each variable. Here, before performing CCA, we reconstructed the initial SST/SIC field based on the first 10 EOF modes, which explain more than 70% of variance in each field (Storch and Zwiers 1999).

One obtains the canonical correlation time series U_i and V_j in term of linear combinations of the EOF time series. After obtaining the canonical correlation time series U_i and V_j, the canonical patterns are derived through linear regression of the time series U_i and V_j onto the original variables, which have been reconstructed using a subset of EOFs (Storch and Zwiers 1999; Zorita et al. 1992):

$$g_j = C_{xx}\alpha_i = \langle U_i, X \rangle$$

$$h_j = C_{yy}\beta_j = \langle V_j, Y \rangle$$

where, g_j and h_j represent the canonical correlation patterns for the variables X and Y respectively. C_{xx} and C_{yy} are the covariance matrices for X and Y, and α_i and β_j are the canonical coefficients. Since U and V are normalized, these patterns reflect the typical amplitude of the associated phenomena in the original data.

CCA is a useful tool to identify the footprint on a field associated with a forcing factor, when distinct drivers are characterized by different temporal evolutions. In our case, distinction between SIC spatial structures, that are associated with either one of increase in atmospheric CO_2 concentration, AMO or NAO, is emphasized based on their specific SST, where SIC and SST are derived in pairs through CCA. In order to validate CCA results across different statistical methods and to infer the physical relevance of the identified coupled patterns, the SAT, SLP, and Surface Wind fields are regressed on the time series from CCA pairs associated with the three specific forcing factors. SAT and SLP fields which are used to obtain the regression maps associated with the AMO were prefiltered with a 5-year running mean in order to remove the inter-annual variability.

The statistical significance of correlations and regression maps is examined in relation to the (two-tailed) probability (p) value to obtain a similar correlation value by chance. Because the significance is affected by the autocorrelation of each time series, the effective number of degrees of freedom N_{ef} used in the calculation is computed with the relation): $N_{ef} = N(1 - R_1 R_2)/(1 + R_1 R_2)$, in which N is the number of values of the time series and R_1, R_2 represent the lag-one autocorrelation of each record (Bretherton et al. 1999).

As the final component of our methodological toolbox we employ Convergent Cross Mapping (CCM). This technique represent a time-embedding reconstruction method that is based on the theory of dynamical systems and that can be used to identify causality between time series (Sugihara et al. 2012). CCM is based on Takens's Theorem (Takens 1981) which states that the E-dimensional dynamics of a multivariate system can be reconstructed from the E-dimensional time embedding of only one variable of the system. Considering the fact that in deterministic dynamical systems effects contain information about causes. Therefore, if X causes Y, then Y can be used to estimate states of X using a time embedding reconstruction. The accuracy to which one can make such a prediction is a measure of causality and it is called cross-mapping. Although cross-mapping is a necessary condition of causality, it is not a sufficient condition. Consequently, causal relationships suggested by cross-mapping must be confirmed by plausibility, for example via identifying physically consistent mechanisms that link a driver with the change it generates. A cross map should increase in accuracy as we add more data to the prediction (increase the library length). At some point the causal information has been fully exploited and there is not more increase in cross map skill, but rather a stabilization at a saturation asymptotic point. This property is called convergence. Pearson's correlation coefficient ρ (here labeled cross map skill) is computed between the observed and predicted time series of the forcing variable. To show convergence, it is plotted against the library length. A combination of convergence and cross-mapping makes CCM a robust method to detect causality in complex systems. Cross-mapping tracks the chain of causality by "running backwards" from the effect Y to the cause X. Thus, a negative lag corresponds to a potential causal direction, while a positive lag violates the causal dogma of causes preceding effects. (Sugihara et al. 2012). This approach is known as Time Delay CCM (TDCCM). We use two randomized surrogate models to test for statistical significance: Ebisuzaki phase shift model (Ebisuzaki 1997) and the Swap method (Van Nes et al. 2015). The Ebisuzaki phase shift model involves computing surrogates of a time series by keeping the same power spectrum of the time series but randomizing the phases. The Swap method chooses a random point in the time series and swaps the divided two segments. This method randomizes the phases but is keeping most of

the local dependencies in the data. We apply the surrogate models on the cause time series and then compute CCM between the observed effect and the surrogate cause. Out of all the surrogate-CCMs we choose the highest 95th one and plot it against the true cross map. If the true cross-map is above the surrogate ones after the convergence point it is deemed statistically significant.

Here, we use CCM in order to show causality between either one of atmospheric CO_2 increase, AMO, and NAO, and the coupled pairs of SST-SIC variability that are identified through CCA. By comparison with randomized surrogate models, we ensure robustness the identified causal links.

4 Results

4.1 Observed coupled pairs of global SST- Arctic SIC variability

Using CCA on observed gridded annual anomalies, we identified coupled patterns of global SST (0–360°, 80°S–80°N latitude) and Arctic SIC (0 to 360°, and 55° to 90°N) fields, extending over the period from 1950 to 2017. The results are presented in Fig. 1 and summarized in Table 1. All three

analyzed pairs pass the degeneracy test (North et al. 1982). The pairs from 4 to 8 do not pass the test for mode degeneracy (Table 1) and are consequently omitted from our study. Additionally, the correlation between the spatial structures significantly decreases after pair 5. SIC changes are occurring primarily at the extremities of the Arctic but not in its central part, where sea ice is still relatively thicker (England et al. 2019). Consistent with this, CCA analysis emphasizes changes in marginal regions of the Arctic and confirms that any changes in SIC over the central Arctic are insignificant. We note that this statement does not hold in a future warmer Arctic, where much less, and much thinner, sea ice will have reduced capacity to similarly dampen sea ice variability than it has today. The time series of the first coupled SST-SIC pair (Fig. 1a) have a correlation coefficient of 0.97 (95% significance level) and show a significant increasing trend throughout the analyzed period. The SST spatial structure of the first CCA pair (Fig. 1d) explains ~41% of the SST variance and is dominated by quasi-uniform positive anomalies, especially pronounced in the Indian Ocean basin, reflecting the recognized SST signature of anthropogenic climate change (Deser et al. 2010). The corresponding SIC pattern (Fig. 1g) accounts for 38% of the variance and is characterized by loss of sea ice across the margins of the Arctic ocean, with pronounced anomalies over the Greenland, Barents, Kara,
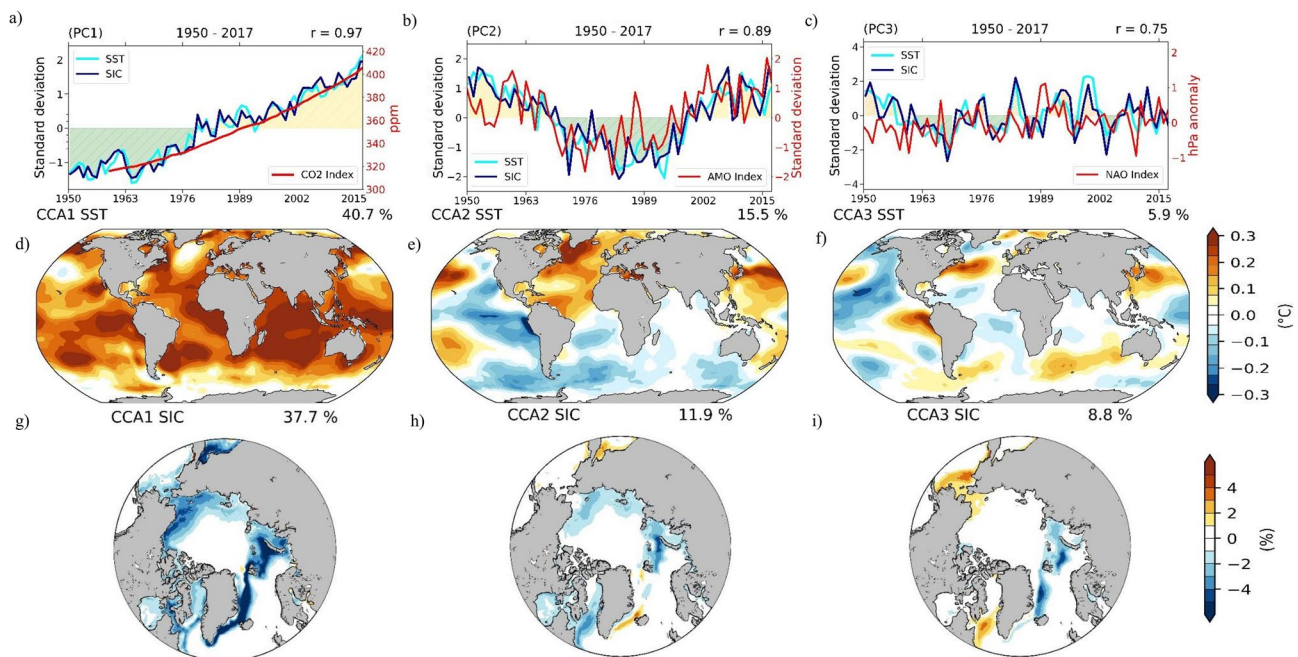
Fig. 1 Coupled global SST (0–360° longitude and −80° to 80° latitude)—Arctic SIC (0–360° longitude and 55–90° latitude) patterns identified through CCA between the corresponding annual fields over the period from 1950–2017. Left column: The time series of the first CCA pair (**a**), with a correlation coefficient of 0.97, together with their associated SST (**d**) and SIC patterns (**g**), explaining 41% and 38% of variance, respectively. **Middle column:** The time series of the second CCA pair (**b**), with a correlation coefficient of 0.89, together with their associated SST (**e**) and SIC patterns (h), explaining 16% and 12% of variance, respectively. Right column: The time series of the third CCA pair (**c**), with a correlation coefficient of 0.75, together with their associated SST (**f**) and SIC patterns (**i**), explaining 16% and 12% of variance, respectively

Table 1 Variances explained by each pattern and significance test for degeneracy for each CCA pair

CCA pair	Variance explained (%) (SST)	Variance explained (%) (SIC)	North test SST	North test SIC	PCs correlation
Pair 1	40.7	37.7	Pass	Pass	0.97
Pair 2	15.5	11.9	Pass	Pass	0.89
Pair 3	5.9	8.8	Pass	Pass	0.75
Pair 4	6.6	7.16	Fail	Pass	0.68
Pair 5	4.7	4.87	Pass	Fail	0.64
Pair 6	7.2	8.47	Fail	Fail	0.47
Pair 7	5.0	7.39	Fail	Fail	0.44
Pair 8	6.8	3.31	Fail	Fail	0.36
Pair 9	0.8	5.53	Fail	Fail	0.25
Pair 10	0.0	4.85	Fail	Fail	0.12
Total	92.7	98.8	–	–	–

Laptev, Beaufort, and Chukchi seas. The observed positive SST values over most of the planetary ocean, the associated SIC pattern, an in-phase Arctic sea-ice oscillation (Wang and Ikeda 2000, 2001), and also the trend in this pair's time series indicate in a convergent way that this coupled pair of SST—SIC variability is closely related to the anthropogenic increase in CO_2 concentration. Most climate models suggests that the significant increase in atmospheric greenhouse gases has been a key driver behind the observed decline in Arctic sea ice in recent decades (Notz and Stroeve 2016; Stroeve and Notz 2018), supporting our attribution.

The time series associated with the second CCA pair (Fig. 1b), have a correlation of 0.89 (95% significance level) and align closely with the AMO Index (r = 0.71, 95% significance level). The SST spatial structure of the second pair (Fig. 1e, 16% of total variance explained) has the maximum loadings over the subpolar gyre and is characterized by positive loadings in the North Atlantic, contrasted by negative anomalies in the South Atlantic, eastern tropical Pacific, Indian, and South Pacific Oceans. This global pattern shows characteristics previously linked to the positive phase of the AMO (Dima and Lohmann 2007; Deser et al. 2010; Ruprich-Robert et al. 2017). In the North Pacific, a Pacific Decadal Oscillation (PDO)-like pattern is observed. The AMO and PDO are not independent from each other (Deser et al. 2010) as it has been shown that AMO can influence the North Pacific SST variability by changing the strength of the Aleutian Low via atmospheric teleconnections AMO (Dima and Lohmann 2007; Zhang and Delworth 2007). The corresponding SIC pattern (Fig. 1f) accounts for 12% of the variance, predominantly showing negative anomalies across the Arctic and Baffin Bay, while positive loadings are observed in the East Greenland Sea.

Both time series from the pairs associated with CO_2 (Fig. 1a) and AMO (Fig. 1b) show an increasing trend since ~1980, a period with a steep decline in Arctic SIC (Cai

et al. 2021b). To assess their impact on SIC over this period, we calculate the mean SIC loadings for both forcing factors over the Arctic (Supp Fig. 7a) and Barents-Kara Seas (Supp. Figure 7b) regions and multiply it with their amplitudes. Our results indicate that the CO_2 increase (CCA Pair 1) exerts a more pronounced influence on sea ice in both cases, with its scaled mean influencing Arctic SIC nearly twice as much as the AMO, emphasizing the importance of CO_2 emissions for recent Arctic SIC changes.

The SST pattern of the third coupled pair (Fig. 1f) accounts for 6% of the global SST variance. This pattern is characterized by positive anomalies to the east of Greenland and in the western sub-tropical North Atlantic, contrasted by negative anomalies over the subpolar gyre and between the equator and 30°N. This tripole pattern spreading over the North Atlantic and Arctic Ocean is generated by the negative phase of the NAO (Hurrell 1995). The NAO is the dominant mode of atmospheric variability in the North Atlantic (Hurrell and Deser 2009) and affects the oceanic surface mainly through changes in turbulent energy fluxes (e.g., Wang et al. 1994, 2004; Marshall et al. 2001; Deser et al. 2010). The corresponding time components (Fig. 1c) are significantly correlated with NAO- Index (r = 0.34, 95% significance level). The dominance of decadal variability in its time series (Fig. 1c) and the North Atlantic tripole-like SST pattern are typical for the Atlantic quasi-decadal mode (Dima et al. 2001). The associated SIC spatial structure (Fig. 1i) explains ~9% of the Arctic SIC variance and has the highest negative loadings over the Barents Sea, while positive loadings are observed over Baffin Bay and the Labrador Sea.

4.2 Associated physical processes

To investigate the physical processes by which the CO_2 increase, the AMO and the NAO manifest their influence

on our coupled SST-SIC pairs identified by CCA, we chose two distinct periods—the melt season, which starts from April to September (A2S), and the freezing season which extends from October to March (O2M), a period when the Arctic SIC is growing. First, we performed a CCA for O2M (Supp. Figure 1) and another CCA for A2S season (Supp. Figure 2). We then regress global surface air temperature (SAT, 0–360° longitude and − 90° to 90° latitude), Northern Hemisphere sea level pressure (SLP, 0–360° longitude and 10–90° latitude), and surface wind (0–360° longitude and 10–90° latitude) fields on the time series from CCA pairs linked with CO_2 increase, AMO, and NAO.

4.2.1 Regression maps for the season of sea ice accumulation (O2M)

The accumulation of Arctic sea ice on time scales beyond the annual cycle is primarily influenced by the amount of heat that is transported to the Arctic region, which can occur either by atmospheric heat transport on interannual time scales (Mysak et al. 1996; Wang et al. 2004; Ding et al. 2019; Olonscheck et al. 2019) and also through oceanic heat transport at decadal to multidecadal intervals (Deser and Teng 2008; Mahajan et al. 2011; Halloran et al. 2020). The

decline in sea ice accumulation in winter as a result of rising temperatures is exacerbated by the uplift and break-up of sea ice in response to wind (Ding et al. 2019; Olonscheck et al. 2019). This process results in newly formed sea ice being more susceptible to melting in summer (Carmack et al. 2015), while the amount of less sensitive perennial sea ice decreases.

The regression map of SAT (Fig. 2a) on SIC time series from the CCA pair associated with the anthropogenic CO_2 forcing shows a significant increase in SAT over vast parts of the Arctic region, a key feature of rising atmospheric CO_2 levels (IPCC AR6 WGI 2021). The relation between an increase in temperature and shrinking Arctic sea ice has previously been linked to changes in atmospheric CO_2 concentration, amplified by their associated positive feedback (Gillett et al. 2008; Notz and Stroeve 2016). The regression map of Northern Hemisphere SLP displays a negative center over the North Pole, surrounded by centers of opposite sign (Fig. 2d). This NAO-like structure brings warm air from the North Atlantic basin towards the East Greenland-Bering-Kara Seas and over Eurasia. This mixed thermally and dynamically induced impacts explain why the SIC structure linked to this forcing over the sea ice accumulation season (Fig. 1g) has its amplitudes over the eastern extremities of
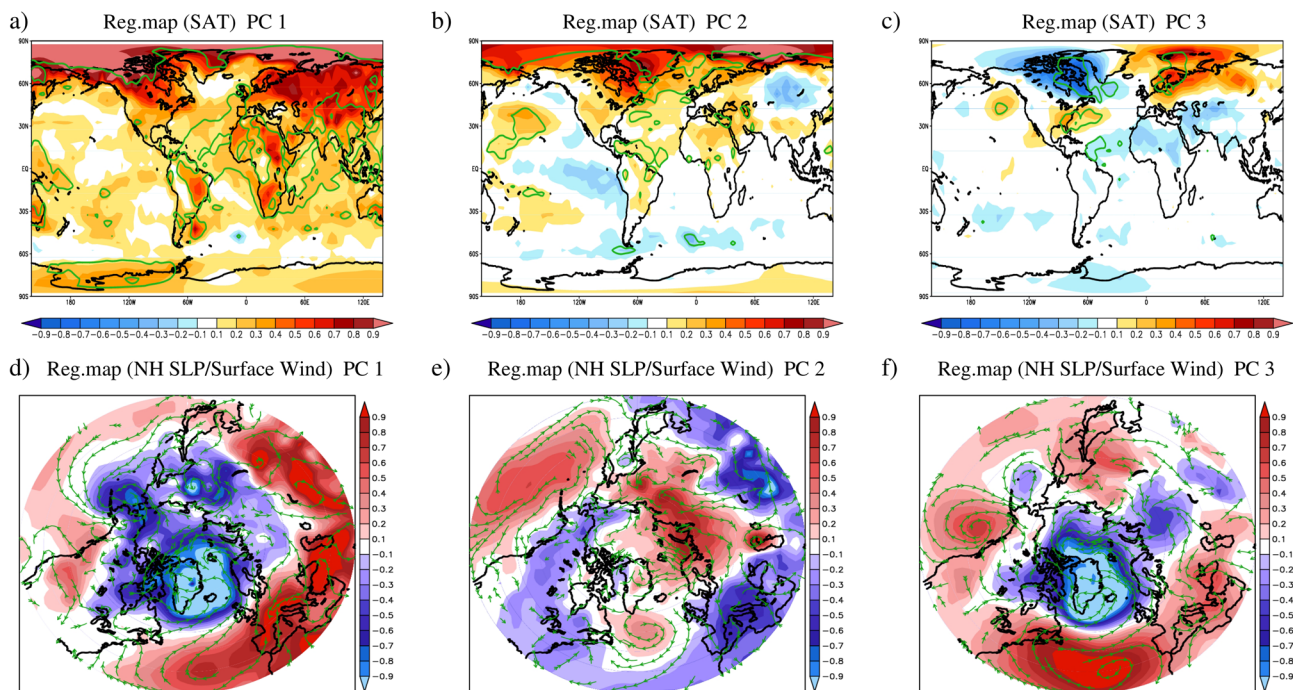
Fig. 2 Associated regression maps for October–March (O2M) season extending over the period from 1950 to 2017. Top row: The regression maps of NCEP/NCAR global surface air temperature (SAT, 0–360° longitude and – 90–90° latitude, °C) on the time series of SST/SIC pair associated to the increase in atmospheric CO_2 (**a**), AMO (**b**) and the NAO (**c**). The associated statistical significance in the highlighted areas (green contours) is above 95%. Bottom row: The regression maps of NCEP/NCAR NH sea level pressure (SLP) (hPa, 0–360° longitude and 10–90° latitude) and surface wind (0° to 360° longitude and 10–90° latitude) on the time series of the SST/SIC pair associated to the increase in atmospheric CO_2 (**d**), AMO (**e**) and NAO (**f**). The associated statistical significance in the highlighted areas (green contours) is above 95%

the Arctic Ocean more intense than over the western part of the Arctic basin. Similarly, the negative loading over the western Arctic are also related to northward advection of relatively warm air from lower latitudes, associated with a local pressure low (Fig. 2d). The CO_2-linked global SLP regression map (Supp. Figure 3a) is characterized by negative loadings in mid-latitude to high-latitude regions and over the poles and by positive values over North Africa and Western Europe, a structure that has been associated with anthropogenic influence by means of observational data and numerical simulations (Gillett et al. 2003, 2013; Vaideanu et al. 2019).

The regression map of SAT on the SIC time series from the SST-SIC pair that is associated to the AMO shows a predominant increase in temperature over North America, North Africa to Europe and over most of the Arctic region and a decrease over Eurasia (Fig. 2b). These characteristics, together with the temperature decrease over the eastern tropical Pacific have been linked with the positive phase of the AMO (Ruprich-Robert et al. 2017). The positive SSTs can be linked with a reduction in the accumulation of sea ice (Latif et al. 2004; Mahajan et al. 2011; Halloran et al. 2020) which in turn generates an increase in temperature (Fang et al. 2022). The physical cause for this effect is linked to the radiative transfer in the climate system, i.e. thinner and less compact sea ice has a different albedo, therefore amplifying the Arctic warming (Chylek et al. 2009). Positive temperatures over the north-eastern Pacific Ocean may be generated by the weakening of the Aleutian Low through weak westerlies (Dima and Lohmann 2007). Over the central-eastern Asia, the AMO generates a decrease in temperature (Knight et al. 2005). The corresponding regression SLP map (Fig. 2e) includes negative values over the mid-Atlantic, consistent with the temperature regression map linked to the AMO (Fig. 2b). The positive SLP over the Arctic may not directly reflect the atmospheric response to local changes in temperature, but rather changes induced by atmospheric teleconnections from the tropics (Yu et al. 2017). The center of positive SLP anomalies located over northern Eurasia (Fig. 2e) implies northward advection of relatively warm air from lower latitudes, which could generate the region of negative SIC anomalies between Laptev Sea and Spitzberd (Fig. 1h). The negative SIC anomalies over the wester Arctic (Fig. 1h) could be linked to the center of positive SLP anomalies located over North Pacific, which implies also northward advection of warm air from lower latitudes (Fig. 2e).

Since the NAO is the predominant atmospheric form in the North Atlantic, as can be seen from the SLP regression map (Fig. 2f), it mainly has thermodynamic effects on the Arctic sea ice (Hurrell and Deser 2009). Over the northern part of the Greenland Sea, the Kara Sea and the southern part of the Laptev Sea, the advection of warm air from the

North Atlantic (Fig. 2f) leads to a decrease in SIC, while over Baffin Bay the cyclonic circulation brings in cold air from the Arctic (Fig. 2c) and thus promotes sea ice growth in this region (Wang et al. 1994; Mysak et al. 1996). Furthermore, the temperature regression map (Fig. 2c) also shows positive values over northern Europe and east of Greenland, and negative values over Baffin Bay and Canada, regions where the NAO has a significant influence (Marshall et al. 2001; Hurrell and Deser 2009).

4.2.2 Regression maps for the period of sea ice melt (A2S)

The SAT, SLP, and surface wind fields regression maps on the SIC time components corresponding to A2S season associated through CCA shown in Fig. 3. Regression maps for SAT are qualitatively similar to those from the O2M season, underscoring, as expected, an anticorrelation between temperature and sea ice cover across the Arctic. The regression map for SLP and CO_2-induced variance (Fig. 3d) differs from that in O2M by lacking the hemispheric zonal symmetry but including a strong zonal gradient in the North Atlantic sector. Positive SLP values are observed over the Arctic region (Fig. 3e), similar with the ones associated with this climate mode in O2M season, which can be related to the tropical teleconnections generated by the AMO (Zhang 2015; Yu et al. 2017). The AMO-induced global SLP regression map shows negative values over the tropical and mid North Atlantic, reflecting the influence from the ocean below (Dima et al. 2001; Buckley and Marshall 2016; Vaideanu et al. 2019) and is in good agreement with previous studies using observations (Vaideanu et al. 2019) and climate model simulations (Ruprich-Robert et al. 2017). The maximum SLP gradient is associated with winds blowing from Northern Europe toward the North Pole In contrast, cold air blows from the Arctic over the East Greenland Sea. Seasonal differences between the SAT and the SLP regression maps that are associated with the AMO can be observed over the north-eastern part of Asia, with the cooling over this region (Knight et al. 2005) being virtually inexistent in this season. The A2S NAO-linked SLP regression map (Fig. 3f) is dominated by the North Atlantic dipolar structure which brings cold air west of Greenland and relatively warm air northward into the Arctic basin along the Scandinavian Peninsula. One notes that the northward wind anomalies corresponding to the North Atlantic SLP gradient associated with the CO_2 increase originate further southward (Fig. 3d) than that one linked with the NAO (Fig. 3f).

4.3 Causal links

The CCA method lacks the means to identify unequivocally causality in the climate system between drivers of variability on the one hand and the emerging patterns of variability on
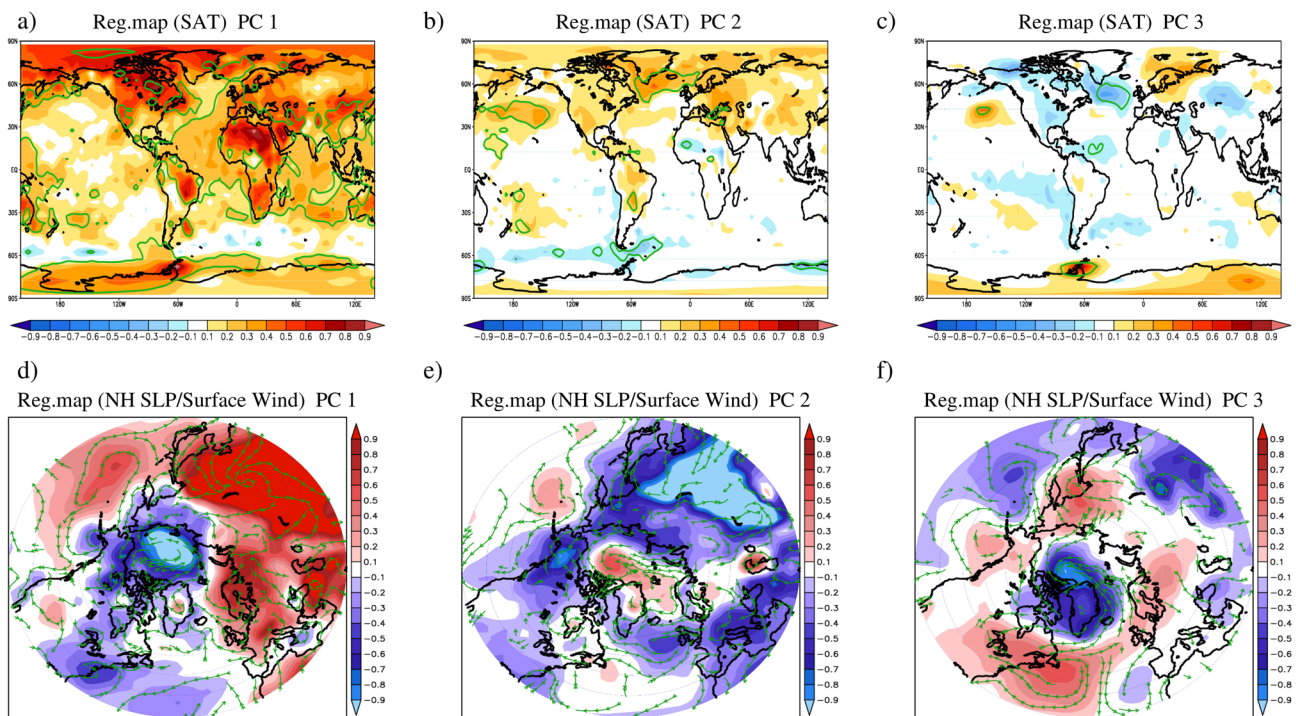
Fig. 3 Associated regression maps for April–September (A2S) season extending over the period from 1950 to 2017. Top row: The regression maps of NCEP/NCAR global surface air temperature (SAT, 0–360° longitude and −90 to 90° latitude, °C) on the time series of the SST/SIC pair associated to increasing atmospheric CO_2 (**a**), AMO (**b**) and NAO (**c**). The associated statistical significance in the highlighted areas (green contours) is above 95%. Bottom row: The regression maps of NCEP/NCAR Northern Hemisphere (NH) sea level pressure (SLP) (hPa, 0–360° longitude and 10–90° latitude) and surface wind (0° to 360° longitude and 10–90° latitude) on the time series of the SST/SIC pair associated to increasing atmospheric CO_2 (**d**), AMO (**e**) and NAO (**f**). The associated statistical significance in the highlighted areas is above 95%

the other hand. To bridge this gap, we employ the CCM method (Sugihara et al. 2012) and test causality between forcing factors and SST and SIC fields after exploring their links with those forcing factors through CCA. The main results are shown in Fig. 4. Cross maps showing causality (red line in all panels), the 95th surrogate under the Ebisuzaki phase-shift model (Ebisuzaki 1997, black line in all panels) and the 95th surrogate under the Swap model (blue line in all panels). All investigated causal relations are in phase (Supp. Figure 5) or have the lag in the interval -(E-1) *$\tau \leq l \leq 0$, where E is the embedding dimension used to make the prediction and τ is the embedding lag (Ye et al. 2015).

First, we analyze the causal relation between CO_2 Index and time series of SST (Fig. 4a) and SIC (Fig. 4b) from the CCA pair that is linked to this forcing. The cross-maps to CO_2 clearly exhibit the highest asymptotic cross-map skill, its performance obviously surpassing the two randomized surrogate models that we use for testing statistical significance. Consequently, we conclude that there is a causal relationship between the increase in atmospheric CO_2 concentration on the one hand and warming of global SST (Fig. 1d) and melting of Arctic SIC (Fig. 1g) on the other hand. We corroborate this finding by repeating this analysis in reverse

direction, i.e., testing causality from PC1_SST to CO_2 and from PC1_SIC to CO_2—in this case a clear and consistent causal signal is absent (Supp. Figure 5, Time Delay CCM).

Given that the AMO is defined as an SST mode, we investigate the causal relation between the SST time series and the SIC time component from the second CCA pair linked to this mode. Figure 4c reveals a compelling causality stemming from PC2_SST towards PC2_SIC. This pronounced causal link supports the attribution of the second observed CCA to the AMO and underscores that its oscillatory warming and cooling phases are a critical determinant in the variability of Arctic SIC.

Since the NAO is primarily an atmospheric climate mode, it has an influence on both the SST and SIC structures from the third CCA pair. Causality from the NAO index to PC3_SST (Fig. 4e) is clear and statistically significant, though milder in strength. Figure 4f presents a slightly nuanced CCM representation, emphasizing causality from the NAO index to PC3_SIC. This nuanced CCM representation may reflect also the different fundamental properties of the two time series: the memory of the SIC record is significantly larger than that of NAO, which is typical for atmospheric records, which contain a significant fraction of noise. While
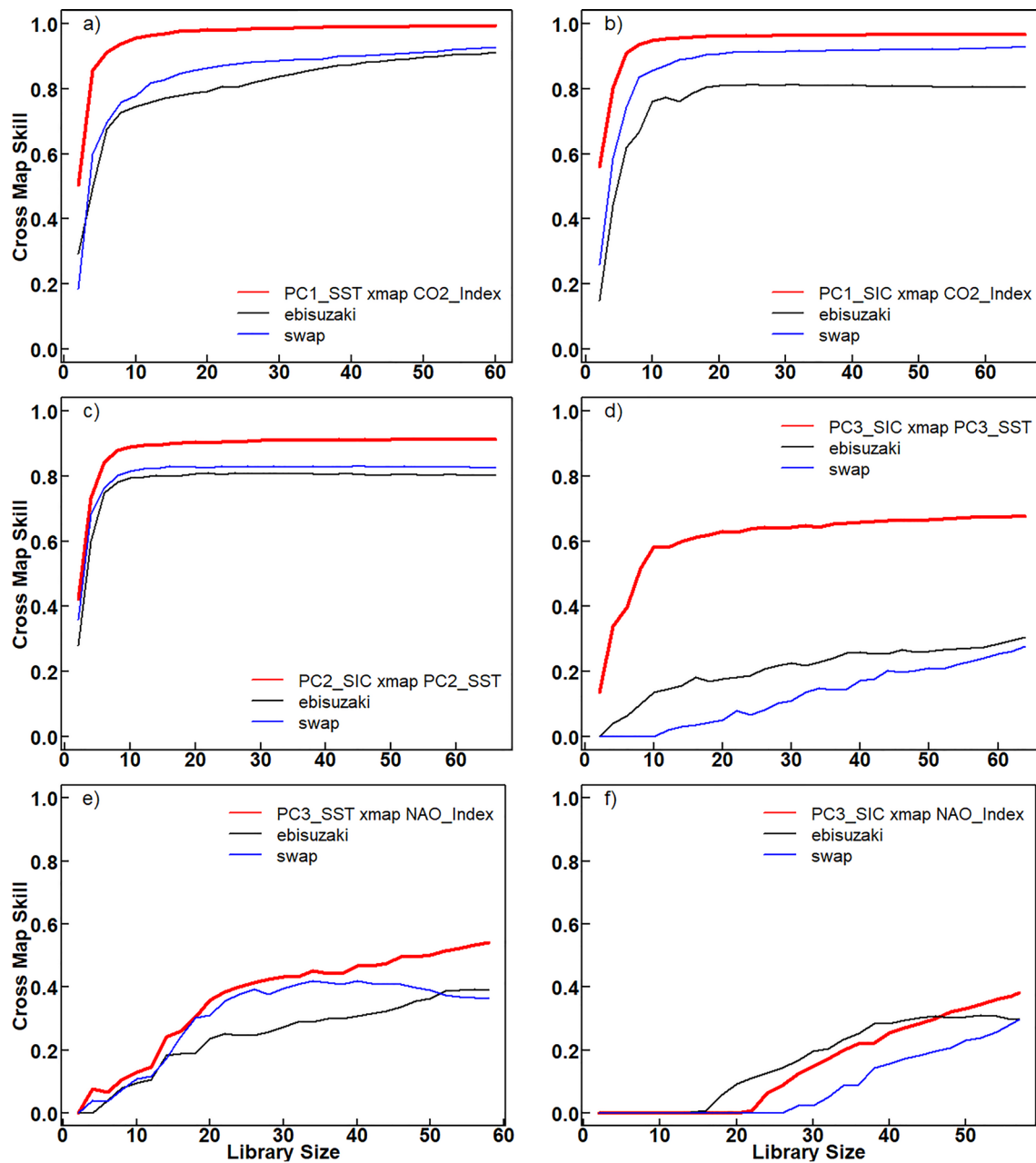
Fig. 4 Causal links between the increase in atmospheric CO_2, the AMO, and the NAO on the one hand and coupled SST-SIC patterns identified through CCA on the other. The cross maps showing causality are represented by the red line in all panels, the black lines represent the 95th surrogate under the Ebisuzaki phase-shift model and the blue lines the 95th surrogate under the Swap model. Panels **a** and **b** display the in-phase statistically significant cross-map from PC1_SST (a) and PC1_SIC (b) to the CO_2 index. Panels **c**) and **d**) show cross estimation from SIC to SST for PC2 with lag 0 (**c**) and PC3 with lag 3 (**d**). Panels **e** and **f** show CCM from SST (**e**) and SIC (**f**) to the NAO index with the lags 0 and 5, respectively

the cross-map is significant under the Swap method, it only reaches statistical significance at the end of the library length for the Ebisuzaki model. This finding suggests that the time series may be too short to establish a robust causal connection. A stronger significant causal link is identified for the causal direction from PC3_SST to PC3_SIC (Fig. 4d), showing that the NAO influence on SIC is manifested primarily through the SST, suggesting that the time series may be too short to establish a robust causal connection. When analyzing the reverse causality direction, we find a significant signal from both the PC3_SST (Supp. Figure 6a) and PC3_SIC (Supp. Figure 6b) to the NAO, highlighting the impact of changes in surface temperature and sea ice on this atmospheric mode of variability.

5 Discussion

As pointed out in the IPCC AR6 Report (2021), there is still no consensus regarding how much of the decline in Arctic sea ice is naturally or anthropogenically driven. In this study we present a multi-faceted perspective on the main drivers of coupled global SST—Arctic SIC variability, combining statistical analysis of observational data with advanced causality testing in order to trace such relationships over the 1950—2017 period.

Towards separating, and comparing the magnitudes, of the influence of atmospheric CO_2 concentrations, of AMO, and of NAO on the coupled SST/SIC fields derived from observations, we apply the CCA method. The identification of all three footprints into the same CCA analysis allows a quantitative estimation of the contributions of the forcing factors to the variability of the coupled global SST-Arctic SIC fields. For a better separation of the three distinct forcing factors, we used global SST and Arctic SIC. The identification of all three footprints via the same CCA analysis allows a quantitative estimation of the contributions of the forcing factors to the variability of the coupled global SST-Arctic SIC fields. However, because the interior Arctic Ocean SIC has much less variability than the marginal zones, the percentage of variance explained by each pair reflect the amount of variance over extremities and not across entire Arctic basin. While the rise in atmospheric CO_2 concentration is the dominant forcing factor, since 1980, the AMO has also been a significant factor in shaping Arctic SIC variability, especially over the Barents-Kara Seas, contributing to its decline, which is about half that caused by rising atmospheric CO_2 concentrations. The pronounced negative SIC anomalies over the Barents and Kara Seas have been previously associated with positive SST anomalies over the North Atlantic, likely reflecting local thermal effects due to northward heat transport (Mahajan et al. 2011; Halloran et al. 2020). In the North Pacific, the warming that is induced by the AMO, generates negative SIC anomalies over the Beaufort, Chukchi, and East Siberian seas, consistent with Arctic sea ice multidecadal variability (Mahajan et al. 2011; Yu et al. 2017). Day et al. (2012) found that natural AMO variability could explain approximately 0.5–3.1% per decade of the 10.1% per decade decline in September SIE between 1979 and 2010, attributing this effect to changes in heat transport from the North Atlantic into the Arctic. In addition to the thermal effect, model simulations suggest that the AMO impacts the formation and evolution of the Arctic SIC also through atmospheric teleconnections from the tropics (Castruccio et al. 2019). Over the southern part of East Greenland Sea, the observed positive SIC anomalies are most likely induced by atmospheric blocking and local changes in the sea ice export through Fram Strait (Ionita et al. 2016). When studying the impact of AMO on, and the causal links with, observed trends in sea ice, the question about the nature of the AMO, and about its drivers, comes to mind. We note that this question has been subject to extensive debate and research (Latif et al. 2004; Dima and Lohmann 2007; Otterå et al. 2010; Booth et al. 2012; Zhang et al. 2013; Murphy et al. 2017; Bellomo et al. 2018; Mann et al. 2021). Our research may not contribute to further elucidating this subject since we have no means to further decompose the AMO into individual drivers. We note, however, that our primary focus is on analyzing the impact of the AMO on coupled SST-SIC variability, irrespective of its underlying nature.

It can be argued that Pacific SST-SIC variability within the NAO-linked pair, resembles with the impact of El Nino Southern Oscillation (ENSO), which is the dominant mode of interannual variability in the Pacific realm (McPhaden et al. 2006; Timmermann et al. 2018; Vaideanu et al. 2023a). The central Pacific mode of ENSO which could be recognized in the SST pattern of the third pair (Fig. 1f) can be interpreted as a response of the Tropical Pacific to the dominant mode of North Atlantic SST variability (Dima et al. 2015). To avoid conflating these influences, our interpretation of this pair focuses specifically on regions where NAO has a stronger, more established impact—namely, Baffin Bay, the Labrador Sea and the Barents Sea. One notes that the time component of the third CCA pair is correlated with the NAO index. Together with the CCM analysis, this correlation is a strong indicator that this pair is linked with NAO. The NAO has been shown to induce changes in surface temperature over the Barents Sea (Hurrell and Deser 2009; Deser et al. 2010; Heukamp et al. 2023), but it can influence the growth of SIC by changing wind patterns in the eastern Arctic Ocean. This increases the sea ice advection out of the Arctic by drifting the sea ice from the center towards its marginal area (Zhang et al. 2003; Strong and Magnusdottir 2010). Over Baffin Bay (Liu et al. 2004; Scholz et al. 2013), and the Labrador Sea (Wang et al. 1994; Mysak et al. 1996), NAO- generates positive SIC anomalies by advecting cold air from the Arctic into this region, thus increasing sea ice accumulation.

CCA results are in line with previous observational data studies based which show that the Arctic sea ice decline observed in the last decades result from a combination of anthropogenic and internal variability (Cai et al. 2021a, b). Minor differences between our and previous work appear regarding the exact value of the percentage of SIC variance that is driven by each attributed forcing factor. These discrepancies can be due to different season chosen for analysis, slightly different prefiltering of the data or due to the different geographic selection. All three CCA pairs derived by us show a significant reduction in SIC over the Barents-Kara Sea, which represents the region experiencing the steepest decline in SIC over the observational period (Cai et al. 2021b). In contrast, Baffin Bay exhibits a less pronounced rate of decline (Cai et al. 2021b), likely due to the opposing impacts of increased CO_2, AMO, and NAO- over this region. This regional response underscores the complexity of

Arctic sea ice dynamics and the need for detailed analyses to quantify and understand the differential impacts of multiple drivers in the region. Recent studies, have highlighted the significant impact of aerosols on Arctic climate, especially in relation to sea ice (Creamean et al. 2022; Fu et al. 2022). Although we acknowledge that the complex aerosol-sea ice link remains an essential aspect of Arctic climate research, we have to note that our attribution to the CCA pairs is based on known global SST patterns, and that we could not identify any CCA pair with an SST pattern that has previously been associated to aerosol influence.

Seasonal regression analyses for SIC melting (A2S) and accumulation (O2M) seasons reveal distinct physical processes linking these fields with the associated forcing. The regression maps and the associated physical processes robustly substantiate the attribution of the three CCA pairs to the impacts of increasing atmospheric CO_2 concentration and of internal variability via AMO and NAO. They are physically consistent with the three coupled SST-SIC pairs. The SAT regression maps are qualitatively similar in A2S and O2M, showing an anticorrelation between temperature and sea ice over the Arctic. Large scale changes in sea ice are affected directly by variations in the energy flux available for growth/melt of the sea ice (Carmack et al. 2015; Stroeve and Notz 2018; Ding et al. 2019; Mioduszewski et al. 2019). Although changes in the energy budget of the atmosphere have been the primary contribution to the decline in Arctic SIC observed in the twentieth century (Olonscheck et al. 2019), it is expected that the contribution through changes in oceanic heat transport will become more prominent in the twenty-first century (Liu and Fedorov 2021).The increase in anthropogenic CO_2 emissions impacts the growth of the Arctic sea ice primarily through its associated increase in temperature but also through advection of warm air from lower latitudes towards the pole via the eastern coast of Greenland, when sea ice is accumulating. The NAO can also induce changes in wind forcing that can induce anomalous sea ice motion in the Arctic, besides the warming of the Barents-Kara seas trough atmospheric heat transport. An important player in the evolution of sea ice in warming climates are feedbacks and processes that change the characteristics of the sea ice and thereby its response to ambient climate. For example, a slowdown in the rate of sea ice accumulation in the growth season will, over time, reduce the thickness of sea ice, making it more vulnerable to changes in atmospheric and oceanic heat transport in summer (Mioduszewski et al. 2019) and to breaking and subsequent transport into warmer regions (Sumata et al. 2023). Furthermore, thinner sea ice has a different albedo and therefore can amplify the summer warming/melting (Chemke et al. 2021). There is a clear seasonal dependency of the impact of warming on sea ice. Regression maps related to the melt season (Fig. 3a and b) show an amplification of Arctic warming, which is the main driver for the melting of Arctic sea ice during this period of the year (Fang et al. 2022). In contrast, for the growth season we find a decrease in the impact induced through the atmosphere, because the atmospheric circulation is not as strong during the growth season as it is during the melt season.

CCM analysis robustly shows causality from rising atmospheric CO_2 concentrations to both global SST warming and Arctic SIC melting. However, when examining the reverse causality, a distinct causal relationship is not evident, as shown in Supp. Figure 5 (Time Delay CCM). CCM shows also pronounced causality from the AMO to SIC underscoring the oceanic influence on Arctic sea ice dynamics. It has been shown that the melting of Arctic sea ice has an influence on the SST multidecadal variability in the North Atlantic (Deng and Dai 2022) but with a lag of ~ 10–30 years (Liu et al. 2019). Therefore, this relation is not suited for our investigation, where we analyze in-phase causal relations and where we, more importantly, do not have observational time series at hand that are of sufficient length. In the case of the NAO, the CCM results reveal a more specific causal influence: while the causality from the NAO index to the SST component is expected and statistically significant, the influence on SIC is more subtle and may require longer time series to establish a robust causal connection. On the other hand, the strength and position of the NAO can also be influenced by the decline in sea ice over the Barents Sea (Wang et al. 2005; Overland and Wang 2010; Kolstad and Screen 2019). This observation is in good agreement with our findings from Supplementary Fig. 6, which highlights the reciprocal influence of SST and SIC on NAO. The causal links identified through CCM validate the physical consistency of dynamical interactions between these different actors and thereby corroborate the relationship that has been suggested by the three coupled CCA patterns and by our interpretation of the physical processes that link these fields.

6 Conclusions

Despite extensive research, the ongoing decline of Arctic sea ice during the last part of the twentieth century remains not fully understood. Our study clearly identifies the effects of variations in atmospheric CO_2 concentration, the AMO and the NAO on the coupled global SST—Arctic SIC variability from 1950 to 2017 and reveals physically consistent relationships between them. Together, the three coupled pairs explain over 50% of the variance in coupled global SST–Arctic SIC fields. Rising CO_2 concentrations are the dominant driver for the observed changes in SST and SIC, underscoring the urgent need for global measures to reduce emissions and mitigate their impact on the Arctic environment. We also show that while greenhouse gas forcing is an important factor for climate change in the Arctic, it is not the sole cause for the observed changes. External forcing is complemented by contributions from two forms of internal

variability known for their relative importance in the North Atlantic-Arctic region. The AMO and the NAO both have the potential to either amplify or attenuate changes caused by anthropogenic forcing, depending on their respective phases. All three influencing factors considered are associated with a significant influence on SIC over the Barents-Kara Sea, a region that has experienced the steepest decline in sea ice in the last 100 years (Cai et al. 2021b) and therefore represents a hotspot of change in Arctic sea ice, being predicted to be the first region to be ice-free in summer (Onarheim et al. 2018). In this region, the positive trend of the AMO since ~ 1980 has contributed substantially to sea ice decline, and its impact is comparable to nearly half of the impact of anthropogenic CO_2 emissions. By establishing robust causal relationships between global SST, Arctic SIC, and these key drivers, we advance understanding of Arctic sea ice variability and offer valuable insights for improving climate model projections. The methodology and results provide a foundation for addressing discrepancies in simulated trends and underscore the urgent need for targeted mitigation strategies to address both anthropogenic and natural contributions to Arctic climate change.

Supplementary Information The online version contains supplementary material available at https://doi.org/10.1007/s00382-025-07623-w.

Data availability All data used in this study is publicly available and all the sources are mentioned in the Methods section.

Code availability The code to perfom CCA and related analyses is publicaly availale on Zenodo: https://doi.org/10.5281/zenodo.10714841. (https://doi.org/https://doi.org/10.5281/zenodo.10714841). The code to perfom CCM is publicly availeble at https://ha0ye.github.io/rEDM/articles/rEDM.html.

Declarations

Conflict of interest The authors have no relevant financial or non-financial interests to disclose.

References

Asbjørnsen H, Årthun M, Skagseth Ø, Eldevik T (2020) Mechanisms underlying recent arctic atlantification. Geophys Res Lett. https://doi.org/10.1029/2020GL088036

Bellomo K, Murphy LN, Cane MA et al (2018) Historical forcings as main drivers of the Atlantic multidecadal variability in the CESM large ensemble. Clim Dyn. https://doi.org/10.1007/s00382-017-3834-3

Bellucci A, Mariotti A, Gualdi S (2017) The role of forcings in the twentieth-century North Atlantic multidecadal variability: the 1940–75 North Atlantic cooling case study. J Clim. https://doi.org/10.1175/JCLI-D-16-0301.1

Bonan DB, Lehner F, Holland MM (2021) Partitioning uncertainty in projections of Arctic sea ice. Environ Res Lett. https://doi.org/10.1088/1748-9326/abe0ec

Booth BBB, Dunstone NJ, Halloran PR et al (2012) Aerosols implicated as a prime driver of twentieth-century North Atlantic climate variability. Nature. https://doi.org/10.1038/nature10946

Bretherton CS, Widmann M, Dymnikov VP et al (1999) The effective number of spatial degrees of freedom of a time-varying field. J Clim 12(7):1990–2009. https://doi.org/10.1175/1520-0442(1999)0122.0.CO;2

Bretones A, Nisancioglu KH, Jensen MF et al (2022) Transient increase in arctic deep-water formation and ocean circulation under sea ice retreat. J Clim. https://doi.org/10.1175/JCLI-D-21-0152.1

Buckley MW, Marshall J (2016) Observations, inferences, and mechanisms of the Atlantic Meridional overturning circulation: a review. Rev Geophys. https://doi.org/10.1002/2015RG000493

Cai Q, Beletsky D, Wang J, Lei R (2021) Interannual and decadal variability of arctic summer sea ice associated with atmospheric

teleconnection patterns during 1850–2017. J Clim. https://doi.org/10.1175/JCLI-D-20-0330.1

Cai Q, Wang J, Beletsky D et al (2021) Accelerated decline of summer Arctic sea ice during 1850–2017 and the amplified Arctic warming during the recent decades. Environ Res Lett. https://doi.org/10.1088/1748-9326/abdb5f

Carmack E, Polyakov I, Padman L et al (2015) Toward quantifying the increasing role of oceanic heat in sea ice loss in the new arctic. Bull Am Meteorol Soc. https://doi.org/10.1175/BAMS-D-13-00177.1

Castruccio FS, Ruprich-Robert Y, Yeager SG et al (2019) Modulation of Arctic Sea ice loss by atmospheric teleconnections from Atlantic multidecadal variability. J Clim. https://doi.org/10.1175/JCLI-D-18-0307.1

Chapman WL, Walsh JE (1993) Recent variations of sea ice and air temperature in high latitudes. Bull Am Meteorol Soc 74(10):33–48. https://doi.org/10.1175/1520-0442(1999)0122.0.CO;2

Chemke R, Polvani LM, Kay JE, Orbe C (2021) Quantifying the role of ocean coupling in Arctic amplification and sea-ice loss over the 21st century. NPJ Clim Atmos Sci. https://doi.org/10.1038/s41612-021-00204-8

Chen HW, Alley RB, Zhang F (2016) Interannual arctic sea ice variability and associated winter weather patterns: a regional perspective for 1979–2014. J Geophys Res. https://doi.org/10.1002/2016JD024769

Cherry S (1996) Singular value decomposition analysis and canonical correlation analysis. J Clim 9(9):2003–2009. https://doi.org/10.1175/1520-0442(1996)0092.0.CO;2

Chylek P, Folland CK, Lesins G et al (2009) Arctic air temperature change amplification and the Atlantic multidecadal oscillation. Geophys Res Lett. https://doi.org/10.1029/2009GL038777

Cohen J, Zhang X, Francis J et al (2020) Divergent consensuses on Arctic amplification influence on midlatitude severe winter weather. Nat Clim Chang. https://doi.org/10.1038/s41558-019-0662-y

Creamean JM, Barry K, Hill TCJ et al (2022) Annual cycle observations of aerosols capable of ice formation in central Arctic clouds. Nat Commun. https://doi.org/10.1038/s41467-022-31182-x

Curry JA, Schramm JL, Serreze MC, Ebert EE (1995) Water vapor feedback over the Arctic Ocean. J Geophys Res. https://doi.org/10.1029/95jd00824

Day JJ, Hargreaves JC, Annan JD, Abe-Ouchi A (2012) Sources of multi-decadal variability in Arctic sea ice extent. Environ Res Lett. https://doi.org/10.1088/1748-9326/7/3/034011

Deng J, Dai A (2022) Sea ice–air interactions amplify multidecadal variability in the North Atlantic and Arctic region. Nat Commun. https://doi.org/10.1038/s41467-022-29810-7

Deser C, Teng H (2008) Evolution of Arctic sea ice concentration trends and the role of atmospheric circulation forcing, 1979–2007. Geophys Res Lett. https://doi.org/10.1029/2007GL032023

Deser C, Alexander MA, Xie S-P, Phillips AS (2010) Sea surface temperature variability: patterns and mechanisms. Ann Rev Mar Sci. https://doi.org/10.1146/annurev-marine-120408-151453

Dima M, Lohmann G (2007) A hemispheric mechanism for the Atlantic multidecadal oscillation. J Clim. https://doi.org/10.1175/JCLI4174.1

Dima M, Rimbu N, Stefan S, Dima I (2001) Quasi-decadal variability in the Atlantic basin involving tropics-midlatitudes and ocean-atmosphere interactions. J Clim. 14(5):823–832

Dima M, Lohmann G, Rimbu N (2015) Possible North Atlantic origin for changes in ENSO properties during the 1970s. Clim Dyn. https://doi.org/10.1007/s00382-014-2173-x

Ding Q, Wallace JM, Battisti DS et al (2014) Tropical forcing of the recent rapid Arctic warming in northeastern Canada and Greenland. Nature. https://doi.org/10.1038/nature13260

Ding Q, Schweiger A, L'Heureux M et al (2019) Fingerprints of internal drivers of Arctic sea ice loss in observations and model simulations. Nat Geosci. https://doi.org/10.1038/s41561-018-0256-8

Divine DV, Dick C (2006) Historical variability of sea ice edge position in the Nordic Seas. J Geophys Res Oceans. https://doi.org/10.1029/2004JC002851

Döscher R, Vihma T, Maksimovich E (2014) Recent advances in understanding the Arctic climate system state and change from a sea ice perspective: a review. Atmos Chem Phys. https://doi.org/10.5194/acp-14-13571-2014

Ebisuzaki W (1997) A method to estimate the statistical significance of a correlation when the data are serially correlated. J Clim. 10(9):2147–53

England M, Jahn A, Polvani L (2019) Nonuniform contribution of internal variability to recent Arctic sea ice loss. J Clim. https://doi.org/10.1175/JCLI-D-18-0864.1

Fang M, Li X, Chen HW, Chen D (2022) Arctic amplification modulated by Atlantic multidecadal oscillation and greenhouse forcing on multidecadal to century scales. Nat Commun. https://doi.org/10.1038/s41467-022-29523-x

Fauria MM, Grinsted A, Helama S et al (2010) Unprecedented low twentieth century winter sea ice extent in the Western Nordic Seas since A.D. 1200. Clim Dyn. https://doi.org/10.1007/s00382-009-0610-z

Folland CK, Knight J, Linderholm HW et al (2009) The summer North Atlantic oscillation: past, present, and future. J Clim. https://doi.org/10.1175/2008JCLI2459.1

Fu Y, Liu P, Tang M (2022) The Arctic sea ice-cloud radiative negative feedback in the Barents and Kara Sea region. Theor Appl Climatol. https://doi.org/10.1007/s00704-022-04137-x

Gillett NP, Zwiers FW, Weaver AJ, Stott PA (2003) Detection of human influence on sea-level pressure. Nature. https://doi.org/10.1038/nature01487

Gillett NP, Stone DA, Stott PA et al (2008) Attribution of polar warming to human influence. Nat Geosci. https://doi.org/10.1038/ngeo338

Gillett NP, Fyfe JC, Parker DE (2013) Attribution of observed sea level pressure trends to greenhouse gas, aerosol, and ozone changes. Geophys Res Lett. https://doi.org/10.1002/grl.50500

Halloran PR, Hall IR, Menary M et al (2020) Natural drivers of multidecadal Arctic sea ice variability over the last millennium. Sci Rep. https://doi.org/10.1038/s41598-020-57472-2

Heukamp FO, Aue L, Wang Q et al (2023) Cyclones modulate the control of the North Atlantic oscillation on transports into the Barents Sea. Commun Earth Environ. https://doi.org/10.1038/s43247-023-00985-1

Hurrell JW (1995) Decadal trends in the North Atlantic oscillation: regional temperatures and precipitation. Science 1979:269. https://doi.org/10.1126/science.269.5224.676

Hurrell JW, Deser C (2009) North Atlantic climate variability: the role of the North Atlantic oscillation. J Mar Syst. https://doi.org/10.1016/j.jmarsys.2008.11.026

Ionita M (2023) The Arctic winter seasons 2016 and 2017: climatological context and analysis. Climate. https://doi.org/10.3390/cli11010019

Ionita M, Scholz P, Lohmann G et al (2016) Linkages between atmospheric blocking, sea ice export through Fram Strait and the Atlantic meridional overturning circulation. Sci Rep. https://doi.org/10.1038/srep32881

Ionita M, Grosfeld K, Scholz P et al (2019) September Arctic sea ice minimum prediction- a skillful new statistical approach. Earth Syst Dyn. https://doi.org/10.5194/esd-10-189-2019

Jungclaus JH, Haak H, Latif M, Mikolajewicz U (2005) Arctic-North Atlantic interactions and multidecadal variability of the meridional overturning circulation. J Clim. https://doi.org/10.1175/JCLI3462.1

Kalnay E, Kanamitsu M, Kistler R et al (1996) The NCEP/NCAR 40-year reanalysis project. Bull Am Meteorol Soc. https://doi.org/10.1175/1520-0477(1996)077%3c0437:TNYRP%3e2.0.CO;2

Kashiwase H, Ohshima KI, Nihashi S, Eicken H (2017) Evidence for ice-ocean albedo feedback in the Arctic Ocean shifting to a seasonal ice zone. Sci Rep. https://doi.org/10.1038/s41598-017-08467-z

Kattsov VM, Ryabinin VE, Overland JE et al (2011) Arctic sea-ice change: a grand challenge of climate science. J Glaciol. https://doi.org/10.3189/002214311796406176

Kay JE, Holland MM, Jahn A (2011) Inter-annual to multi-decadal Arctic sea ice extent trends in a warming world. Geophys Res Lett. https://doi.org/10.1029/2011GL048008

Kerr RA (2000) A North Atlantic climate pacemaker for the centuries. Science. https://doi.org/10.1126/science.288.5473.1984

Knight JR, Allan RJ, Folland CK et al (2005) A signature of persistent natural thermohaline circulation cycles in observed climate. Geophys Res Lett 32:1–4. https://doi.org/10.1029/2005GL024233

Kolstad EW, Screen JA (2019) Nonstationary relationship between autumn Arctic sea ice and the winter North Atlantic oscillation. Geophys Res Lett. https://doi.org/10.1029/2019GL083059

Latif M, Roeckner E, Botzet M et al (2004) Reconstructing, monitoring, and predicting multidecadal-scale changes in the North Atlantic thermohaline circulation with sea surface temperature. J Clim. 17(7):1605–14

Lei R, Tian-Kunze X, Leppäranta M et al (2016) Changes in summer sea ice, albedo, and portioning of surface solar radiation in the Pacific sector of Arctic Ocean during 1982–2009. J Geophys Res Oceans. https://doi.org/10.1002/2016JC011831

Letterly A, Key J, Liu Y (2016) The influence of winter cloud on summer sea ice in the Arctic, 1983–2013. J Geophys Res. https://doi.org/10.1002/2015JD024316

Levine RA, Wilks DS (2000) Statistical methods in the atmospheric sciences. J Am Stat Assoc. https://doi.org/10.2307/2669579

Liu W, Fedorov A (2021) Interaction between Arctic sea ice and the Atlantic meridional overturning circulation in a warming climate. Clim Dyn. https://doi.org/10.1007/s00382-021-05993-5

Liu J, Curry JA, Hu Y (2004) Recent Arctic sea ice variability: connections to the Arctic oscillation and the ENSO. Geophys Res Lett. https://doi.org/10.1029/2004GL019858

Liu W, Fedorov A, Sévellec F (2019) The mechanisms of the Atlantic meridional overturning circulation slowdown induced by Arctic sea ice decline. J Clim. https://doi.org/10.1175/JCLI-D-18-0231.1

Liu W, Fedorov AV, Xie SP, Hu S (2020) Climate impacts of a weakened Atlantic meridional overturning circulation in a warming climate. Sci Adv. https://doi.org/10.1126/sciadv.aaz4876

Lorenz EN (1956) Empirical Orthogonal Functions and Statistical Weather Prediction. Technical report Statistical Forecast Project Report 1 Department of Meteorology MIT 49

Mahajan S, Zhang R, Delworth TL (2011) Impact of the atlantic meridional overturning circulation (AMOC) on arctic surface air temperature and sea ice variability. J Clim. https://doi.org/10.1175/2011JCLI4002.1

Mann ME, Steinman BA, Brouillette DJ, Miller SK (2021) Multidecadal climate oscillations during the past millennium driven by volcanic forcing. Science 1979:371. https://doi.org/10.1126/science.abc5810

Marshall J, Johnson H, Goodmann J (2001) A study o f the interaction of the North Atlantic oscillation with ocean circulation. J Clim 14(7):1399–1421. https://doi.org/10.1175/1520-0442(2001)0142.0.CO;2

McPhaden MJ, Zebiak SE, Glantz MH (2006) ENSO as an integrating concept in earth science. Science. 314:1740–1745. https://doi.org/10.1126/science.1132588

Meier WN, Hovelsrud GK, Van Oort BEH et al (2014) Arctic sea ice in transformation: a review of recent observed changes and impacts on biology and human activity. Rev Geophys. https://doi.org/10.1002/2013RG000431

Miles MW, Divine DV, Furevik T et al (2014) A signal of persistent Atlantic multidecadal variability in Arctic sea ice. Geophys Res Lett. https://doi.org/10.1002/2013GL058084

Mioduszewski JR, Vavrus S, Wang M et al (2019) Past and future inter-annual variability in Arctic sea ice in coupled climate models. Cryosphere. https://doi.org/10.5194/tc-13-113-2019

Mueller BL, Gillett NP, Monahan AH, Zwiers FW (2018) Attribution of Arctic sea ice decline from 1953 to 2012 to influences from natural, greenhouse gas, and anthropogenic aerosol forcing. J Clim. https://doi.org/10.1175/JCLI-D-17-0552.1

Murphy LN, Bellomo K, Cane M, Clement A (2017) The role of historical forcings in simulating the observed Atlantic multidecadal oscillation. Geophys Res Lett. https://doi.org/10.1002/2016GL071337

Mysak LA, Ingram RG, Wang J, Van Der Baaren A (1996) The anomalous sea-ice extent in Hudson bay, Baffin bay and the Labrador sea during three simultaneous NAO and ENSO episodes. Atmos Ocean. https://doi.org/10.1080/07055900.1996.9649567

North GR, Bell TL, Cahalan RF, Moeng FJ (1982) Sampling errors in the estimation of empirical orthogonal functions. Mon Weather Rev 110(7). https://doi.org/10.1175/1520-0493(1982)1102.0.CO;2

Notz D, Stroeve J (2016) Observed Arctic sea-ice loss directly follows anthropogenic CO2 emission. Science. https://doi.org/10.1126/science.aag2345

Notz D, Stroeve J (2018) The trajectory towards a seasonally ice-free Arctic ocean. Curr Clim Change Rep. https://doi.org/10.1007/s40641-018-0113-2

Olonscheck D, Mauritsen T, Notz D (2019) Arctic sea-ice variability is primarily driven by atmospheric temperature fluctuations. Nat Geosci. https://doi.org/10.1038/s41561-019-0363-1

Onarheim IH, Eldevik T, Smedsrud LH, Stroeve JC (2018) Seasonal and regional manifestation of Arctic sea ice loss. J Clim. https://doi.org/10.1175/JCLI-D-17-0427.1

Otterå OH, Bentsen M, Drange H, Suo L (2010) External forcing as a metronome for Atlantic multidecadal variability. Nat Geosci. https://doi.org/10.1038/ngeo955

Overland JE, Wang M (2010) Large-scale atmospheric circulation changes are associated with the recent loss of Arctic sea ice. Tellus Series A Dyn Meteorol Oceanogr. https://doi.org/10.1111/j.1600-0870.2009.00421.x

Rayner NA, Parker DE, Horton EB et al (2003) Global analyses of sea surface temperature, sea ice, and night marine air temperature since the late nineteenth century. J Geophys Res d: Atmos. https://doi.org/10.1029/2002jd002670

Ruprich-Robert Y, Msadek R, Castruccio F et al (2017) Assessing the climate impacts of the observed Atlantic multidecadal variability using the GFDL CM2.1 and NCAR CESM1 global coupled models. J Clim. https://doi.org/10.1175/JCLI-D-16-0127.1

Schlesinger ME, Ramankutty N (1994) An oscillation in the global climate system of period 65–70 years. Nature. https://doi.org/10.1038/367723a0

Scholz P, Lohmann G, Wang Q, Danilov S (2013) Evaluation of a finite-element sea-ice ocean model (FESOM) set-up to study the interannual to decadal variability in the deep-water formation rates. Ocean Dyn. https://doi.org/10.1007/s10236-012-0590-0

Screen JA, Francis JA (2016) Contribution of sea-ice loss to Arctic amplification is regulated by Pacific Ocean decadal variability. Nat Clim Chang. https://doi.org/10.1038/nclimate3011

Serreze MC, Meier WN (2019) The Arctic's sea ice cover: trends, variability, predictability, and comparisons to the Antarctic. Ann NY Acad Sci. https://doi.org/10.1111/nyas.13856

Serreze MC, Holland MM, Stroeve J (2007) Perspectives on the Arctic's shrinking sea-ice cover. Scienc. https://doi.org/10.1126/science.1139426

Stein R, Fahl K, Schreck M et al (2016) Evidence for ice-free summers in the late Miocene central Arctic Ocean. Nat Commun. https://doi.org/10.1038/ncomms11148

Stroeve J, Notz D (2018) Changing state of Arctic sea ice across all seasons. Environ Res Lett. https://doi.org/10.1088/1748-9326/aade56

Strong C, Magnusdottir G (2010) Modeled winter sea ice variability and the North Atlantic oscillation: a multi-century perspective. Clim Dyn. https://doi.org/10.1007/s00382-009-0550-7

Sugihara G, May R, Ye H et al (2012) Detecting causality in complex ecosystems. Science 1979:338. https://doi.org/10.1126/science.1227079

Sumata H, de Steur L, Divine DV et al (2023) Regime shift in Arctic ocean sea ice thickness. Nature. https://doi.org/10.1038/s41586-022-05686-x

Sutton RT, Hodson DLR (2005) Ocean science: Atlantic ocean forcing of North American and European summer climate. Science. https://doi.org/10.1126/science.1109496

Svendsen L, Keenlyside N, Bethke I et al (2018) Pacific contribution to the early twentieth-century warming in the Arctic. Nature Clim Change 8:793–797. https://doi.org/10.1038/s41558-018-0247-1

Swart NC, Fyfe JC, Hawkins E et al (2015) Influence of internal variability on Arctic sea-ice trends. Nat Clim Chang. https://doi.org/10.1038/nclimate2483Takens

Thompson DWJ, Wallace JM (2000) Annular modes in the extratropical circulation. Part I: month-to-month variability. J Clim. 13(5):1000–16

Timmermann A, An S-I, Kug J-S et al (2018) El Niño-Southern oscillation complexity. Nature 559:535–545. https://doi.org/10.1038/s41586-018-0252-6

Vaideanu P, Dima M, Voiculescu M (2018) Atlantic Multidecadal Oscillation footprint on global high cloud cover. Theor Appl Climatol. https://doi.org/10.1007/s00704-017-2330-3

Vaideanu P, Dima M, Pirloaga R, Ionita M (2019) Disentangling and quantifying contributions of distinct forcing factors to the observed global sea level pressure field. Clim Dyn. https://doi.org/10.1007/s00382-019-05067-7

Vaideanu P, Ionita M, Voiculescu M, Rimbu N (2023) Deconstructing global observed and reanalysis total cloud cover fields based on pacific climate modes. Atmosphere (Basel). https://doi.org/10.3390/atmos14030456

Vaideanu P, Stepanek C, Dima M et al (2023) Large-scale sea ice-Surface temperature variability linked to Atlantic meridional overturning circulation. PLoS One. https://doi.org/10.1371/journal.pone.0290437

Van Nes EH, Scheffer M, Brovkin V et al (2015) Causal feedbacks in climate change. Nat Clim Chang. https://doi.org/10.1038/nclimate2568

Vermassen F, O'Regan M, de Boer A et al (2023) A seasonally ice-free Arctic ocean during the last interglacial. Nat Geosci. https://doi.org/10.1038/s41561-023-01227-x

von Storch H, Zwiers FW (1999) Statistical analysis in climate research. Cambridge University Press, Cambridge. https://doi.org/10.1017/CBO9780511612336

Walsh JE, Johnson CM (1979) An analysis of Arctic sea ice fluctuations, 1953–77. J Phys Oceanogr 9(3):580–591. https://doi.org/10.1175/1520-0485(1979)0092.0.CO;2

Walsh JE, Fetterer F, Scott Stewart J, Chapman WL (2017) A database for depicting Arctic sea ice variations back to 1850. Geogr Rev 107:89–107. https://doi.org/10.1111/j.1931-0846.2016.12195.x

Walsh JE, Chapman WL, Fetterer F (2015) Gridded Monthly Sea Ice Extent and Concentration, 1850 Onward, Version 1. Boulder, CO. National Snow and Ice Data Center Digital media NSIDC: National Snow and Ice Data Center. https://doi.org/10.7265/N5833PZ5

Wang J, Ikeda M (2000) Arctic oscillation and Arctic sea-ice oscillation. Geophys Res Lett 27:1287–1290. https://doi.org/10.1029/1999GL002389

Wang J, Ikeda M (2001) Arctic sea-ice oscillation: regional and seasonal perspectives. Ann Glaciol 33:481–492. https://doi.org/10.3189/172756401781818626

Wang J, Mysak LA, Grant Ingram R (1994) Interannual variability of sea-ice cover in hudson bay, baffin bay and the Labrador sea. Atmos Ocean. https://doi.org/10.1080/07055900.1994.9649505

Wang J, Wu B, Tang CCL et al (2004) Seesaw structure of subsurface temperature anomalies between the Barents Sea and the Labrador Sea. Geophys Res Lett. https://doi.org/10.1029/2004GL019981

Wang J, Ikeda M, Zhang S, Gerdes R (2005) Linking the northern hemisphere sea-ice reduction trend and the quasi-decadal arctic sea-ice oscillation. Clim Dyn. https://doi.org/10.1007/s00382-004-0454-5

Wei W, Lohmann G (2012) Simulated atlantic multidecadal oscillation during the holocene. J Clim. https://doi.org/10.1175/JCLI-D-11-00667.1

Wu A, Hsieh WW, Shabbar A et al (2006) The nonlinear association between the Arctic Oscillation and North American winter climate. Clim Dyn. https://doi.org/10.1007/s00382-006-0118-8

Ye H, Deyle ER, Gilarranz LJ, Sugihara G (2015) Distinguishing time-delayed causal interactions using convergent cross mapping. Sci Rep. https://doi.org/10.1038/srep14750

Yu L, Zhong S, Winkler JA et al (2017) Possible connections of the opposite trends in Arctic and Antarctic sea-ice cover. Sci Rep. https://doi.org/10.1038/srep45804

IPCC, 2021:Climate Change 2021: The Physical Science Basis. Contribution of Working Group I to the Sixth Assessment Report of the Intergovernmental Panel on Climate Change[Masson-Delmotte, V., P. Zhai, A. Pirani, S.L. Connors, C. Péan, S. Berger, N. Caud, Y. Chen, L. Goldfarb, M.I. Gomis, M. Huang, K. Leitzell, E. Lonnoy, J.B.R. Matthews, T.K. Maycock, T. Waterfield, O. Yelekçi, R. Yu, and B. Zhou (eds.). Cambridge University Press, Cambridge, United Kingdom and New York, NY, USA, In press. https://doi.org/10.1017/9781009157896

Zhang R (2015) Mechanisms for low-frequency variability of summer Arctic sea ice extent. Proc Natl Acad Sci USA. https://doi.org/10.1073/pnas.1422296112

Zhang R, Delworth TL (2007) Impact of the Atlantic multidecadal oscillation on North pacific climate variability. Geophys Res Lett. https://doi.org/10.1029/2007GL031601

Zhang X, Ikeda M, Walsh JE (2003) Arctic sea ice and freshwater changes driven by the atmospheric leading mode in a coupled sea ice-ocean model. J Clim. 16(13):2159–77

Zhang R, Delworth TL, Dixon KW et al (2013) Have aerosols caused the observed atlantic multidecadal variability? J Atmos Sci. https://doi.org/10.1175/JAS-D-12-0331.1

Zhang R, Sutton R, Danabasoglu G et al (2019) A review of the role of the Atlantic meridional overturning circulation in Atlantic multidecadal variability and associated climate impacts. Rev Geophys 57:316–375. https://doi.org/10.1029/2019RG000644

Zhong W, Cole ST, Zhang J et al (2022) Increasing winter ocean-to-ice heat flux in the beaufort Gyre region, Arctic ocean over 2006–2018. Geophys Res Lett. https://doi.org/10.1029/2021GL096216

Zorita E, Kharin V, Von Storch H (1992) The atmospheric circulation and sea surface temperature in the North Atlantic area in winter: their interaction and relevance for Iberian precipitation. J Clim 5. https://doi.org/10.1175/1520-0442(1992)0052.0.CO;2